Gain-Enhanced Planar Log-Periodic Dipole Array Antenna Using Nonresonant Metamaterial

Guohua Zhai, Xi Wang, Rensheng Xie, Jin Shi, Jianjun Gao, Bo Shi, and Jun Ding

***Abstract*— In this communication, a novel nonresonant metamaterial (MTM) structure is proposed to enhance the gain of the clamped-mode planar log-periodic dipole array (CMPLPDA) antenna fed by substrate integrated waveguide. The proposed MTM structures composed of a series of metallic semiring patches are printed on both sides of the antenna substrate, featuring low loss, broadband, and easy integration. Different arrangements of the nonresonant MTM with respect to the dipoles of the CMPLPDA antenna are investigated and compared. The proposed gain-enhanced method based on the nonresonant MTM has been studied through both numerical simulations and experiments. Compared to the original CMPLPDA antenna without any MTM inclusions, the proposed CMPLPDA antenna fully loaded with nonresonant MTM inclusions exhibits a gain enhancement of at least 1.6 dB (up to 4 dB at 27 GHz) within the operating band of 26–40 GHz in the simulations, which is also validated by the experiments.**

***Index Terms*— Clamped-mode planar log-periodic dipole array (CMPLPDA) antenna, gain enhancement, nonresonant metamaterial (MTM), substrate integrated waveguide.**

I. Introduction

Recently, more and more attention has been paid on the wideband directional antenna designs because of the pervasive application of modern wireless communications. The log-periodic dipole array (LPDA) antenna has occupied considerable applications with the characteristics of low profile, stable radiation, and wideband [1]–[3]. However, the traditional LPDA antenna suffers from low directivity and large dimensions. Therefore, there has been of great interest in realizing high gain planar LPDA (PLPDA) antennas [4]–[8]. A conventional effective way of enhancing the antenna gain is to form an array, which might pose the drawbacks of enlarged size, high cost and losses, and design complexity [5]. Besides, the linear directors were added into the PLPDA antenna to improve the gain [9], which could only take effect at the high frequencies. Furthermore, the clamped-mode PLPDA (CMPLPDA) antenna was proposed for the gain enhancement with a similar radiation property of a 1×2 PLPDA antenna array [10]. However, the gain-increasing methods discussed above have little effect on the PLPDA antenna at low-end frequency band, which degrades the gain flatness of the antenna within the whole operating band. Thus, it is necessary to develop novel technologies for broadband gain enhancement, especially for the low-end frequency band.

The isotropic near-zero index metamaterial (NZIM) structures have been applied to embed into the antenna for gain enhancement. Several meander-line structures were reported to improve the gain of directional antennas, e.g., the Vivaldi antenna and the antipodal tapered slot antenna [12]–[14]. In addition, I-shaped resonant structure was utilized to enhance the gain of the quasi-Yagi antenna [15]. However, the resonant metamaterial (MTM) structures might limit the antenna bandwidth and introduce more losses due to the strong dispersions. In order to lower the losses, a nonresonant MTM was considered in a highly efficient broadband PLPDA antenna [16].

In this communication, to further enhance the gain of the super high gain CMPLPDA antenna [10] within a wide bandwidth, a novel nonresonant MTM structure is proposed and loaded into the CMPLPDA antenna while keeping all other performances almost intact. Featuring low loss and broadband, the nonresonant unit cell consisting of a semiring patch is first proposed, designed, and optimized. In the whole operating *Ka*-band, the real parts of the retrieved refractive index and relative permittivity are almost constant and greater than unity, respectively, while both the imaginary parts approach zero. Then, the effects of the proposed MTM structure with different locations on the CMPLPDA antenna are first studied by numerical simulations. It is demonstrated that the gain of the optimized MTM-loaded CMPLPDA antenna could be increased by 1.6–4 dB within the operating *Ka*-band with the identical size of the original CMPLPDA antenna. Accordingly, the gain flatness of the CMPLPDA antenna is greatly improved. Then, a conventional CMPLPDA antenna and two MTM-loaded CMPLPDA antennas are fabricated and characterized. The measured results agree very well with the simulated results, which validates the effectiveness of the proposed gain enhancement method by using the nonresonant MTM structure. In the end, a short conclusion is provided.

II. Nonresonant Metamaterial

To realize a nonresonant electrical and magnetic response, nonresonant MTMs are generally engineered by simple structures, such as metal blocking lines and metal thin circular rings [15], [16]. For simple design and easy fabrication, a novel planar nonresonant MTM unit cell composed of a semiring patch printed on a substrate is proposed, the schematic of which is shown in Fig. 1(a). The width and radius of the semiring patch are denoted as w and r, respectively, and L_g and W_d are the periodicities in the z- and x-directions, respectively.

Manuscript received May 3, 2018; revised April 20, 2019; accepted May 6, 2019. Date of publication June 26, 2019; date of current version September 4, 2019. This work was supported in part by the Natural Science Foundation of Shanghai under Grant 16ZR1445800, in part by the Open Foundation of the State Key Laboratory of Millimeter Waves under Grant 201621, in part by the Shanghai Key Laboratory of Multi-dimensional Information Processing East China Normal University, in part by the Shanghai Pujiang Program under Grant 18PJ1403200, in part by Fundamental Research Funds for Central Universities, and in part by Economic Development Board (EDB), Singapore, through the Space Research Programme under Grant S14-1138-IAF and Grant S15-1322-IAF OSTIN-SIAG. *(Corresponding author: Jun Ding.)*

G. Zhai is with the Information Science and Technology Department, East China Normal University, Shanghai 200241, China, and also with the Institute for Infocomm Research, A∗STAR, Singapore 138632 (e-mail: ghzhai@ee.ecnu.edu.cn).

X. Wang, R. Xie, J. Gao, and J. Ding are with the Information Science and Technology Department, East China Normal University, Shanghai 200241, China (e-mail: jding@ee.ecnu.edu.cn).

J. Shi is with the School of Electronics and Information, Nantong University, Nantong 226019, China.

B. Shi is with the Institute for Infocomm Research, A∗STAR, Singapore 138632 (e-mail: shibo@i2r.a-star.edu.sg).

Color versions of one or more of the figures in this communication are available online at http://ieeexplore.ieee.org.

Digital Object Identifier 10.1109/TAP.2019.2924111

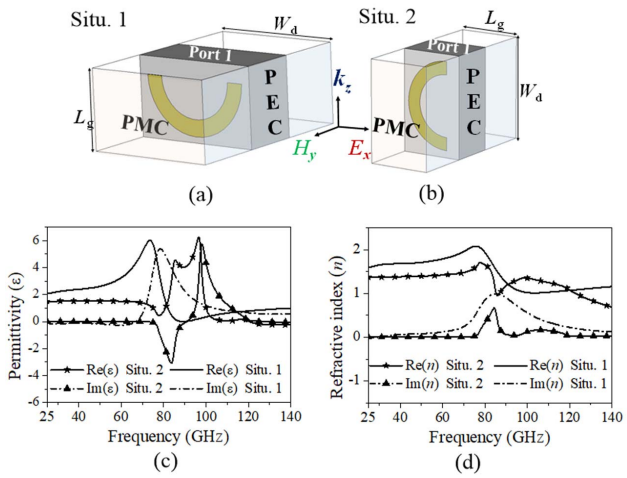

Fig. 1. Two simplified situations for the wave propagating in the z-direction and the E-field parallel to the semiring patch. (a) Situ. 1. (b) Situ. 2. (c) Retrieved relative permittivity for both Situ. 1 and Situ. 2. (d) Retrieved refractive index for both Situ. 1 and Situ. 2.

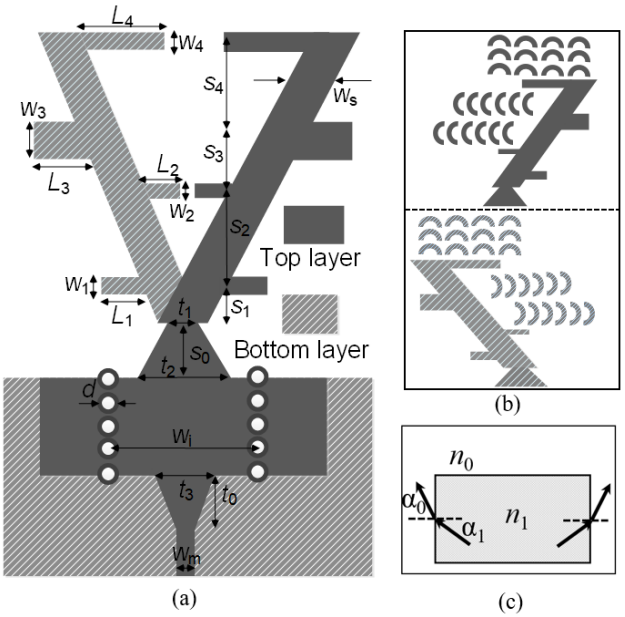

Fig. 2. (a) Geometry of the CMPLPDA antenna. (b) Top and bottom surfaces of the CMPLPDA antenna without SIW. (c) Theoretical model of the proposed nonresonant MTM.

In order to characterize the proposed MTM, an air-filled waveguide with a unit cell placed at its center is modeled. As the incident wave propagating along z-direction is the main interest in this design, two simplified situations (i.e., Situ. 1 and Situ. 2), as shown in Fig. 1(a) and (b), can occur. In the unit cell simulations, the ports are perpendicular to the propagating z-direction. Fig. 1(a) and (b) demonstrates Port 1 on the top surface, which is one of the two ports. In order to make the E-field in the xoz plane, the left and right surfaces of the waveguide are assigned as perfect electric walls and the other two sides as perfect magnetic walls, as shown in both Fig. 1(a) and (b).

The proposed nonresonant MTM structure is printed on a single-layer Rogers RT5880 substrate with a thickness of 0.5 mm and a permittivity of 2.2. For working at Ka-band, the dimensions are chosen as (unit: mm): $w = 0.14$ (0.15 λ_0, λ_0 is the free wavelength at the center frequency of 35 GHz), $r = 0.47$ (0.52 λ_0), $L_g = 0.67$ (0.73 λ_0), and $W_d = 1.14$ (1.2 λ_0). The retrieved refractive index and effective permittivity with respect to the frequency for both situations are shown in Fig. 1(c) and (d), respectively. The effective electromagnetic parameters of the nonresonant MTM unit are calculated from scattering parameters using the inversion method [17], and Kramers–Kronig relationship is adopted to solve the problem of fuzzy solutions and confirm the uniqueness of the solution [18]. As seen from the results, the values of imaginary parts of these constitutive parameters are approximately zero from 26 to 40 GHz, which indicates that the loss of the MTM is negligible. Within the operating band of 26–40 GHz shown as the shadow areas in Fig. 1(c) and (d), the real parts of the effective permittivity and refractive index for Situ. 1 (Situ. 2) are almost constant being about 2.1 (1.8) and 1.5 (1.34), respectively.

III. Gain-Enhanced CMPLPDA Antenna Loaded With Metamaterial Structure

As mentioned in [10], the performance of the SIW CMPLPDA antenna is similar to that of the 1 × 2 parallel PLPDA antenna array, but the CMPLPDA antenna only poses half size of the 1 × 2 array. Fig. 2(a) shows the geometry of the SIW CMPLPDA antenna including the tapered microstrip transition. Similar to the PLPDA antenna element, the CMPLPDA antenna has two feeding lines distributed on both top and bottom layers, which are inclined to form a clamped angle between them. Thus, the antenna in Fig. 2(a) is shaped to be a clamp, which is called a clamped-mode PLPDA antenna [10].

In this communication, an SIW CMPLPDA antenna is designed and optimized to work at the Ka-band, which is printed on both sides of a single-layer Rogers RT5880 substrate with a thickness of 0.5 mm. According to the design principle in [10] by using the full-wave software HFSS, the detailed dimensions of the SIW CMPLPDA antenna are optimized as (unit: mm): $W_1 = 0.3$, $W_2 = 0.3$, $W_3 = 1.1$, $W_4 = 0.15$, $L_1 = 0.8$, $L_2 = 0.63$, $L_3 = 1.75$, $L_4 = 2.17$, $S_1 = 0.55$, $S_2 = 1.35$, $S_3 = 2.09$, $S_4 = 1.64$, $t_0 = 1.4$, $t_1 = 0.4$, $t_2 = 2.6$, $t_3 = 1.92$, $d = 0.3$, $W_i = 4.8$, $W_m = 1.5$, and $W_s = 1.3$.

Fig. 2(b) shows the top and bottom surfaces of the CMPLPDA antenna without the SIW part, which are mirror images to each other along the centerline. As seen from the sketches, the proposed unit cells can be arranged on the side and/or the top of the log-periodic dipoles. The theoretical model of the proposed nonresonant MTM can be simplified in Fig. 2(c). According to Snell's law, the relationship between the incident angle α_1 and refraction angle α_0 upon an interface is given by

$$n_1 \times \sin\alpha_1 = n_0 \times \sin\alpha_0 \tag{1}$$

where $n_1 > 1$ and $n_0 = 1$ are the refractive indexes of the dielectric and air, respectively. From (1), it can be seen that the refraction angle α_1 is mainly determined by the refractive indexes of the two media when illuminated by a plane wave. As discussed earlier, the refractive index of the proposed MTM structure is around 1.5 for Situ. 1 (1.34 for Situ. 2) across the whole operating Ka-band, thus the refraction angle α_0 is larger than the incident angle α_1, which makes the transmitted wave bend toward the centerline, and therefore, the gain of the CMPLPDA antenna can be enhanced.

To investigate the gain enhancement capability of the proposed nonresonant MTM, the CMPLPDA antennas loaded with/without MTM are simulated and compared. Fig. 3 shows the top layers of six different CMPLPDA antennas for gain enhancement study. The electric field distributions could have strongly interfered nearby the dipoles, such as in Regions A and B in Fig. 3. In considering the

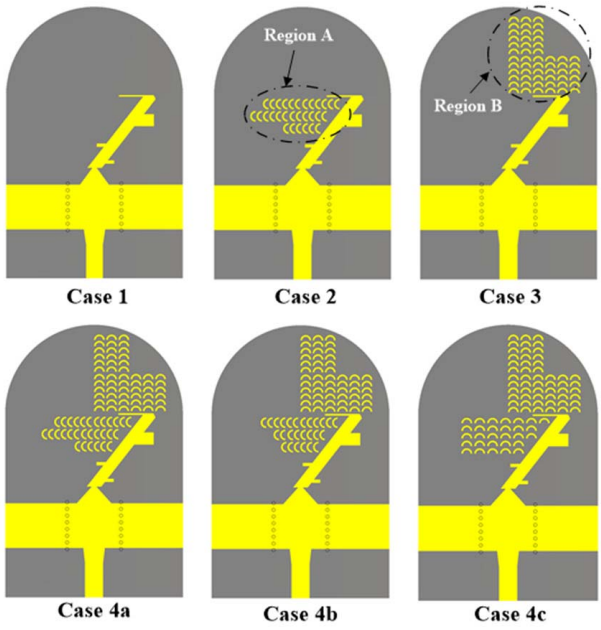

Fig. 3. Configuration of the top layer of the antenna prototypes with different distribution of the MTM inclusions.

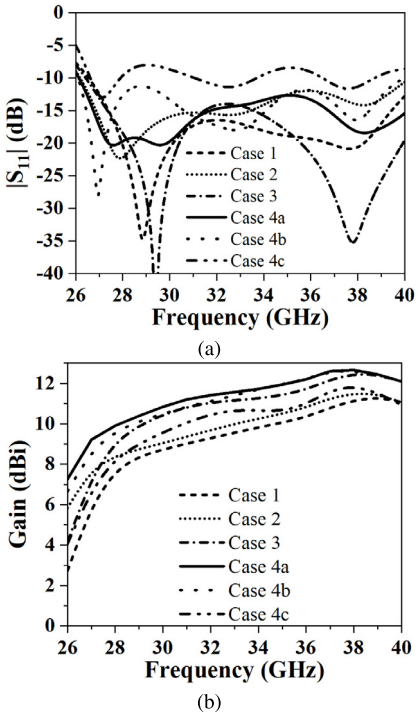

Fig. 4. Simulated (a) $|S_{11}|$ and (b) gains of the four different cases of the PLPDA antenna.

arrangement of the MTM inclusions in these two regions, we tried to place as many unit cells as possible to mimic the periodic boundary condition for an infinite array. Besides, as indicated in (1), the MTM inclusions possessing a higher refractive index are preferred. Therefore, the distributions of the MTM inclusions in Regions A and B are finally determined as shown in Cases 2 and 3 of Fig. 3, respectively. Case 4a is the fully loaded case, which is the combination of Cases 2 and 3. In addition, different arrangements in Region A are also investigated (i.e., Cases 4b and 4c).

The six cases shown in Fig. 3 are defined as follows.

1) Case 1: The original CMPLPDA antenna prototype without MTM.
2) Case 2: The MTM is situated on the left (right) side (i.e., Region A) of the top (bottom) dipole of the CMPLPDA antenna. The MTMs on top and bottom surfaces are inserted between the two dipoles of the CMPLPDA antenna.
3) Case 3: The MTM is situated above the top dipole (i.e., Region B) of the CMPLPDA antenna, which could be used to guide the transmitted wave to the propagation direction.
4) Case 4a: The MTMs are situated on both the sides and above the dipoles of the CMPLPDA antenna, which is the combination of Cases 2 and 3.
5) Case 4b: Similar organization of the MTM inclusions as that in Case 4a with a reduced number of the unit cell in the second row of the MTM inclusions in Region A.
6) Case 4c: Compared to Case 4a, the MTM inclusions in Region A are rotated by 90°, clockwise.

Fig. 4(a) and (b) shows the simulated $|S_{11}|$ and gains of the six CMPLPDA antennas, respectively. It can be seen that the simulated $|S_{11}|$ for all six cases except for Case 4c are less than -10 dB within the operating band of 26–40 GHz. Compared to the original CMPLPDA antenna (Case 1), the $|S_{11}|$ of the five MTM-loaded CMPLPDA antennas except Case 4c demonstrate very slight differences. Meanwhile, over the frequency band of 26.5–40 GHz, the simulated gain profile of Case 1 is 4–11.3 dB, which is the reference for the gain-enhancement comparisons. For Case 2, i.e., the MTMs are situated on the sides of the dipoles of the CMPLPDA antenna, obvious gain enhancement can be observed at low-end frequency band while slight improvement is obtained at high-end frequency band. Compared with the antenna gain of Case 1, not only is the antenna gain of Case 2 enhanced but the gain fluctuation is also improved. In addition, compared to Case 2, the antenna gain for Case 3 is a little smaller in the frequency band lower than 27.5 GHz and then is increased up by 1.8 dB in the frequency range from 27.5 to 40 GHz. For Case 4a, i.e., the combination of Cases 2 and 3, the gain enhancement is around the superposition of the two cases, which is verified by simulation as shown in Fig. 4(b). For Case 4b, as shown in Fig. 4(b) that the gain enhancement is reduced a little at low-end frequency band (from around 26–34 GHz) compared to that for Case 4a. While for Case 4c, the matching is not well as shown in Fig. 4(a). Besides, Fig. 4(b) shows that the gain enhancement for Case 4c is less than that for Case 4a (down by at least 1 dB over the whole operating frequency range). Therefore, in the following study, Cases 1, 2, 3, and 4a are considered.

In summary, for Case 2, the MTM exhibits significant influence on the antenna gain at a lower frequency from 26 to 29 GHz. For Case 3, the gain is uniformly enhanced within the whole operating band. For Case 4a, the antenna enhancement varies from 1 to 4 dB, and the gain fluctuation is improved from 5.3 to 3.4 dB across the band of 26–40 GHz, which could benefit the efficiency of the wireless system.

Fig. 5 shows the E-field distributions of the above-mentioned four cases. For simplicity, two typical frequencies of 28 and 38 GHz are chosen. It is clearly shown that the E-field distributions become uniform and intense by loading the designed semiring patches on the antenna.

IV. Fabrication and Experiment

In this section, the proposed gain enhancement method using the novel nonresonant MTM is validated through experiments. For proof of concept demonstrations, the prototypes of the CMPLPDA antennas

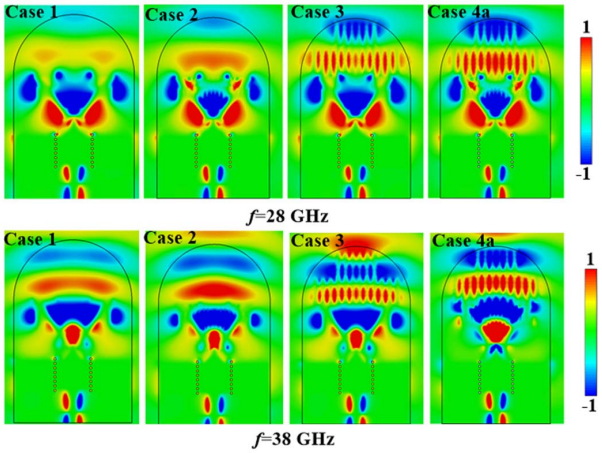

Fig. 5. E-field distributions of four cases at 28 and 38 GHz for comparison.

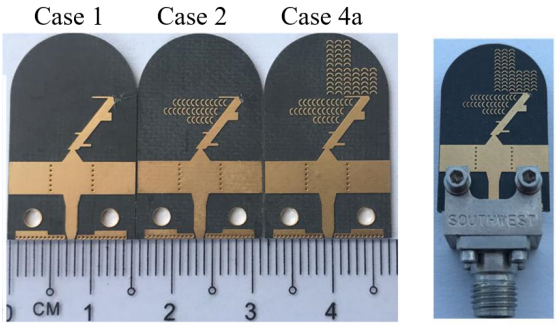

Fig. 6. Top view of the photographs of the CMPLPDA antennas for Cases 1, 2, and 4a, and the CMPLPDA antenna for Case 4a with the end-launcher.

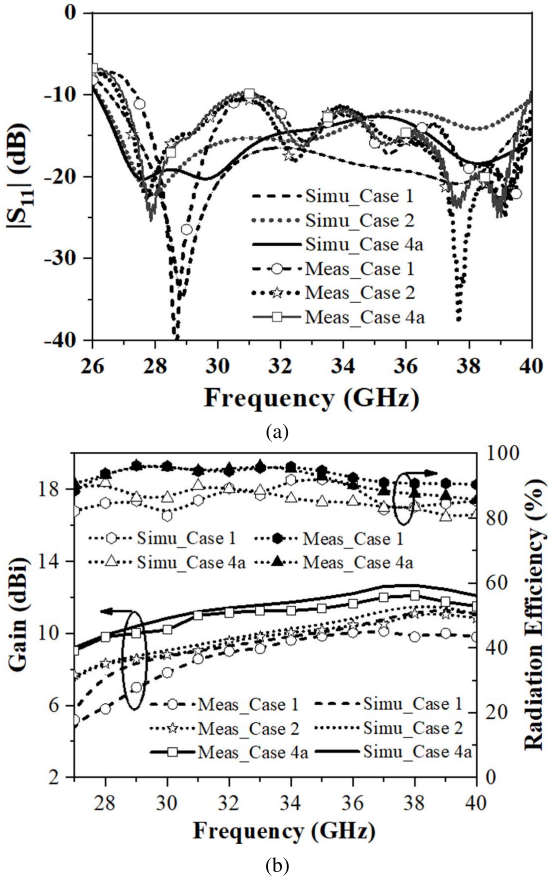

Fig. 7. Measured and simulated (a) $|S_{11}|$ of the CMPLPDA antennas for Cases 1, 2, and 4a, and (b) gain and efficiency of the CMPLPDA antennas for Cases 1 and 4a.

for Cases 1, 2, and 4 are fabricated on the substrate of Rogers RT5880 with a thickness of 0.5 mm. Fig. 6 shows the photographs for these three cases. The parameters of the three antennas are identical with each other except the distributions of the MTM, which are listed in Section III. The overall size of the PLPDA antenna is 15 mm $\times$ 22 mm $\times$ 0.5 mm.

At high frequency, especially millimeter-waves, the increase in both the signal leakage and connector losses will greatly disable the measurement when using traditional SMAs. In order to achieve a precise and reliable test, the end-launch connector is a good choice for the measurement of planar circuits and antennas, which could enable the measurement setup up to 110 GHz. As shown in Fig. 6, a simple feeding microstrip-to-connector transition is designed according to the principle proposed in [19]. It comprises a tapered microstrip, ground pads, and vias. The tapered microstrip is used to match the impedance between the connector and the antenna. The ground pads and vias contribute to the protection of the inner pin of the connector and the reduction of the RF signal leakage. As an example, the CMPLPDA antenna (Case 4a) with the end-launcher for measurement is presented. All the following measured results include the losses of microstrip lines, the feeding microstrip-to-connector transition, and the end-launch connectors.

The measured $|S_{11}|$ of the three antennas are shown in Fig. 7(a). As shown in Fig. 7(a), the measured results agree very well with the simulated results in Fig. 4(a) and the $|S_{11}|$ are less than -10 dB within the band of 27–40 GHz. The slight frequency shift may be caused by the effects of the measurement environment, the end-launcher connectors, and the frequency-dependent permittivity of the substrate, which is not considered in the full-wave simulations.

The measured gains of the antennas are shown in Fig. 7(b), which once again agree very well with the simulated results in Fig. 4(b). It is further verified that the MTM inserted between the dipoles of the CMPLPDA antenna has an obvious effect on the antenna gain at low-end frequency band (lower than 31 GHz). Compared to Case 1, the antenna gain enhancement of Case 2 is up to 2.5 dB, while a maximum gain increment of 4 dB can be obtained for Case 4a. Based on the modified Wheeler Cap method [20], the simulated and measured radiation efficiencies of the antennas for Cases 1 and 4a across the band of 26–40 GHz are also shown in Fig. 7(b), which are about 80%.

For all three fabricated antennas, the far-field radiation patterns in both E-/H-planes (*xoz*/*yoz* planes as shown in Fig. 2) are recorded across the band of 26–40 GHz with a step of 1 GHz. The CMPLPDA antennas loaded with the MTM still feature the endfire radiation patterns within the operating frequency band, which is confirmed by the measurement. For simplicity, only the measured far-field patterns at 30, 34, and 38 GHz are presented in Fig. 8. The measured front-to-back ratios are lower than 15 dB in both E-plane and H-plane within the whole operating frequency band.

The half-power beamwidth (HPBW) and sidelobe level (SLL) of the antennas for both Cases 1 and 4a are shown in Fig. 9. Over the band of 27–40 GHz, the SLL of the antenna for Case 4a becomes better at both the lower-end and higher-end bands and poorer in the middle. The maximum SLLs in the E-/H-planes will be lower than -10 and -8 dB, respectively, which can be further

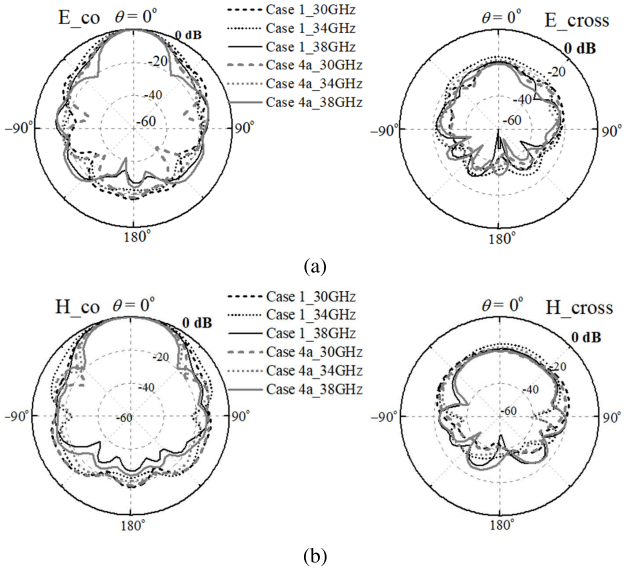

Fig. 8. Normalized copol/cross-pol patterns of the CMPLPDA antennas with/without MTM. (a) E-plane. (b) H-plane. (E/H_co: copolarization in E-/H-planes, E/H_cross: cross polarization in E-/H-planes.)

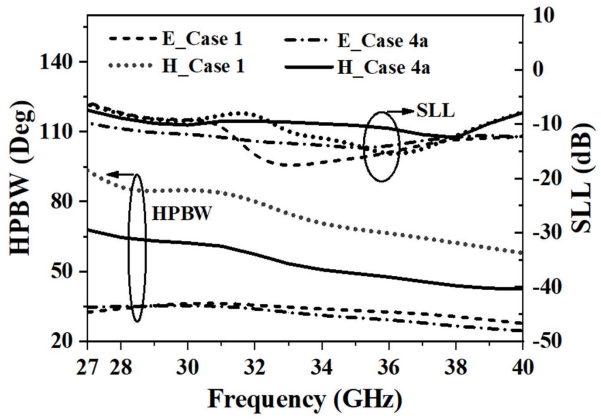

Fig. 9. Comparisons of the HPBW and SLL for the PLPDA antennas for Cases 1 and 4a.

TABLE I

COMPARISON BETWEEN THE PROPOSED ANTENNA AND PREVIOUS REPORTED PLPDA ANTENNA DESIGN

Ref	Band (GHz)	Gain (dBi)	Size (λ_L^3)
[8]	8.4-14.6	6.5-9.5	0.7×2.1×0.022
[9]	21-40	6-10.9	1.28×2×0.035
[10]	26-40	5.8-11	1.28×1.51×0.043
[21]	2-18	7.5-9	0.67×1.93×0.003
[22]	13-20	10-12	1×1.9×0.3
[23]	40-50	7.3-12.5	0.75×2.33×0.067
This work	26-40	6.7-12.3	1.3×2×0.043

λ_L is the wavelength at the lowest frequency of passband

improved by optimizing the width of the ground working as a reflector [5]. By loading with the MTM, the cross polarization of the CMPLPDA antenna is slightly improved by about 1.8 dB at boresight as the MTM improves the current purity along x-direction for the dipoles.

Several PLPDA antennas reported in past years are summarized in Table I with respect to the working band, gain, and size. As shown in Table I, the proposed antenna can be considered as a high gain directional antenna compared to the reported PLPDA antennas, especially the antenna in [10] which is claimed to be "super high gain."

To summarize, the gain of the CMPLPDA antenna can be further enhanced within the whole operating *Ka*-band by loading with the proposed MTM structures. Specifically, the maximum gain increment of the CMPLPDA antenna fully loaded with MTM (Case 4a) is about 4 dB compared with the original CMPLPDA antenna (Case 1) at 27 GHz. Therefore, the loaded MTM inclusions could overcome the limits of both the printed Log-Yagi dipole array antenna [9] and CMPLPDA antenna [10], which could effectively enhance the antenna gain only at higher frequency band. Accordingly, the proposed MTM can greatly improve the gain flatness of the planar-type LPDA antennas within a broad bandwidth, which could bring benefits of high efficiency, reliability, and low power consumption for the wireless communication system.

V. CONCLUSION

To conclude, a novel nonresonant MTM structure composed of semiring patches is proposed to further enhance the gain of a super high gain CMPLPDA antenna without sacrificing any other critical performances. The retrieved material properties of the proposed MTM unit cell have indicated that the real part of the effective refractive index is larger than unity and almost constant over the operating band of 27–40 GHz, while the imaginary part of the effective refractive index approaches zero in the operating band. The proposed nonresonant MTM structure can improve both the gain and gain flatness of the CMPLPDA antenna within a broad bandwidth. The CMPLPDA antennas loaded with different distributed MTM structures are investigated through both simulation and experiment, and three CMPLPDA antennas prototypes (labeled as Cases 1, 2, and 4a) are fabricated and characterized. The measured results of the three antennas agree very well with the simulated ones. Compared to the original CMPLPDA antenna (Case 1), the proposed antenna (Case 4a) presents a gain enhancement of at least 1.6 dB (up to 4 dB at 27 GHz) and a gain-flatness improvement of 2.1 dB over the whole operating band. The proposed method could be of great interest to the wireless communication systems.

REFERENCES

[1] E. C. Jordan and R. W. P. King, "Advances in the field of antennas and propagation since world war II: Part I—Antennas," *Proc. IRE*, vol. 50, no. 5, pp. 705–706, May 1962.

[2] W.-M. Cheong and R. W. P. King, "Log-periodic dipole antenna," *Radio Sci.*, vol. 2, no. 11, pp. 1315–1325, Nov. 1967.

[3] C. C. Bantin and K. G. Balmain, "Study of compressed log-periodic dipole antennas," *IEEE Trans. Antennas Propag.*, vol. 18, no. 2, pp. 195–203, Mar. 1970.

[4] R. Pantoja, A. Sapienza, and F. M. Filho, "A microwave printed planar log-periodic dipole array antenna," *IEEE Trans. Antennas Propag.*, vol. 35, no. 10, pp. 1176–1178, Oct. 1987.

[5] G. H. Zhai, W. Hong, K. Wu, and Z. Q. Kuai, "Wideband substrate integrated printed log-periodic dipole array antenna," *IEE Proc. Microw., Antennas Propag.*, vol. 4, no. 7, pp. 899–905, Jul. 2010.

[6] G. H. Zhai, Y. Cheng, D. Min, S. Z. Zhu, and J. J. Gao, "Wideband simplified feed for printed log-periodic dipole array antenna," *Electron. Lett.*, vol. 49, no. 23, pp. 1430–1432, Nov. 2013.

[7] T. Ma, J. Ai, M. Shen, and W. T. Joines, "Design of novel broadband endfire dipole array antennas," *IEEE Antennas Wireless Propag. Lett.*, vol. 16, pp. 2935–2938, 2017.

[8] X. Wei, J. Liu, and Y. Long, "Printed log-periodic monopole array antenna with a simple feeding structure," *IEEE Antennas Wireless Propag. Lett.*, vol. 17, no. 1, pp. 58–61, Jan. 2018.

[9] G. Zhai, Y. Cheng, Q. Yin, S. Z. Zhu, and J. Gao, "Gain enhancement of printed log-periodic dipole array antenna using director cell," *IEEE Trans. Antennas Propag.*, vol. 62, no. 11, pp. 5195–5199, Nov. 2014.

[10] G. Zhai, Y. Cheng, Q. Yin, L. Chiu, S. Zhu, and J. Gao, "Super high gain substrate integrated clamped-mode printed log-periodic dipole array antenna," *IEEE Trans. Antennas Propag.*, vol. 61, no. 6, pp. 3009–3016, Jun. 2013.

[11] B. Zhou and T. J. Cui, "Directivity enhancement to vivaldi antennas using compactly anisotropic zero-index metamaterials," *IEEE Antennas Wireless Propag. Lett.*, vol. 10, pp. 327–329, 2011.

[12] M. Sun, Z. N. Chen, and X. Qing, "Gain enhancement of 60-GHz antipodal tapered slot antenna using zero-index metamaterial," *IEEE Trans. Antennas Propag.*, vol. 61, no. 4, pp. 1741–1746, Apr. 2013.

[13] H. Zhou *et al.*, "A novel high-directivity microstrip patch antenna based on zero-index metamaterial," *IEEE Antennas Wireless Propag. Lett.*, vol. 8, pp. 538–541, 2009.

[14] R. Haghpanahan and R. Nilavalan, "Planar quasi-Yagi antenna gain enhancement using zero-index metamaterials," in *Proc. Loughborough Antennas Propag. Conf. (LAPC)*, Nov. 2014, pp. 736–739.

[15] R. Liu, Q. Cheng, J. Y. Chin, J. J. Mock, T. J. Cui, and D. R. Smith, "Broadband gradient index microwave quasi-optical elements based on non-resonant metamaterials," *Opt. Express*, vol. 17, no. 23, pp. 21030–21041, Nov. 2009.

[16] X.-Y. He *et al.*, "Nonresonant metamaterials with an ultra-high permittivity," *Chin. Phys. Lett.*, vol. 28, no. 5, Dec. 2010, Art. no. 057701.

[17] X. Chen, T. M. Grzegorczyk, B.-I. Wu, J. Pacheco, Jr., and J. A. Kong, "Robust method to retrieve the constitutive effective parameters of metamaterials," *Phys. Rev. E, Stat. Phys. Plasmas Fluids Relat. Interdiscip. Top.*, vol. 70, no. 1, Jul. 2004, Art. no. 016608.

[18] Z. Szabo, G.-H. Park, R. Hedge, and E.-P. Li, "A unique extraction of metamaterial parameters based on Kramers–Kronig relationship," *IEEE Trans. Microw. Theory Techn.*, vol. 58, no. 10, pp. 1451–1461, Oct. 2010.

[19] Southwest Microwave. *Optimizing Test Boards for 50 GHz End Launch Connectors*. Accessed: Jul. 7, 2019. [Online]. Available: https://mpd.southwestmicrowave.com/documentation/

[20] R. H. Johnston and J. G. McRory, "An improved small antenna radiation-efficiency measurement method," *IEEE Antennas Propag. Mag.*, vol. 40, no. 5, pp. 40–48, Oct. 1998.

[21] Q. Chen, Z. Hu, Z. Shen, and W. Wen, "2-18 GHz conformal low-profile log-periodic array on a cylindrical conductor," *IEEE Trans. Antennas Propag.*, vol. 66, no. 2, pp. 729–736, Feb. 2017.

[22] Y.-X. Zhang, Y.-C. Jiao, and S.-B. Liu, "3-D-printed comb mushroom-like dielectric lens for stable gain enhancement of printed log-periodic dipole array," *IEEE Trans. Antennas Propag.*, vol. 17, no. 11, pp. 2099–2103, Nov. 2018.

[23] Q.-X. Chu, X.-R. Li, and M. Ye, "High-gain printed log-periodic dipole array antenna with parasitic cell for 5G communication," *IEEE Trans. Antennas Propag.*, vol. 65, no. 12, pp. 6338–6344, Dec. 2017.